*J. Phycol.* **37,** 143–159 (2001)

# EVOLUTION OF *PHACUS* (EUGLENOPHYCEAE) AS INFERRED FROM PELLICLE MORPHOLOGY AND SSU rDNA[1]

*Brian S. Leander*[2] *and Mark A. Farmer*

Center for Advanced Ultrastructural Research, 154 Barrow Hall, The University of Georgia, Athens, Georgia, 30602

**This research integrates a large morphological data set into a molecular context. Nineteen pellicle characters and 62 states from 13 euglenid taxa were analyzed cladistically. The pellicle morphology of *Euglena tripteris* (Klebs), *Lepocinclis ovata* (Conrad), *Phacus brachykentron* (Pochmann), *P. oscillans* (Klebs), *P. pyrum* (Stein), and *P. triqueter* (Dujardin) is described comprehensively. These data are compared with new information on the pellicle morphology of *Euglena acus* (Ehrenberg), *E. stellata* (Mainx), and *Peranema trichophorum* (Stein) in addition to published data on *Entosiphon sulcatum* (Dujardin), *Euglena gracilis* (Klebs), *Distigma proteus* (Pringsheim), and *Petalomonas cantuscygni* (Cann and Pennick). Nuclear small subunit (SSU) rDNA sequences provided an independent test for establishing a robust organismal pedigree of the same taxa. A synthetic tree derived from the combined phylogenetic analyses of pellicle morphology and SSU rDNA enabled us to parsimoniously map morphological character states. This approach demonstrated the utility of pellicle morphology for inferring phylogenetic relationships of euglenids and establishing apomorphy-based clade definitions. Three robust clades with unambiguous pellicle-based apomorphies can be recognized within taxa traditionally classified as *Phacus*: (1) *L. ovata* and *P. pyrum*, (2) *E. tripteris* and *P. triqueter*, and (3) *P. brachykentron* and *P. oscillans*. Taxonomic concerns that emerged from these results are discussed.**

*Key index words: Euglena*; Euglenophyta; Euglenozoa; evolution; *Lepocinclis*; pellicle; *Phacus*; phylogeny; taxonomy

*Abbreviations:* **P, the maximum number of strips around the cell periphery; S, the number of strips between consecutively terminating strips; SSU, small subunit; T, the number of strips that converge at the posterior tip; $W_A$, the number of whorls at the anterior end; $W_P$, the number of whorls at the posterior end**

The taxonomic history of euglenids has included many classification systems that were based primarily on a limited number of morphological characteristics observable with light microscopy (Klebs 1883, Bütschli 1884, Senn 1900, Lemmermann 1913, Calkins 1933, Hollande 1942, 1952). The classification most often used today (Leedale 1967, 1978) incorporates some physiological information and ultrastructural data. Even though the classification system proposed by Leedale (1967) was a significant improvement over previous schemes, limited awareness of euglenid characteristics continues to forestall phylogenetic hypotheses with predictive power. New molecular and morphological data have accrued over the past 15 years, indicating that the current set of taxonomic problems within the Euglenida is profound (Farmer 1988, Linton et al. 1999, Linton et al. 2000, Preisfeld et al. 2000).

Euglenids have been lumped informally into two groups depending on the general state of the pellicle, namely the "aplastic" and the "plastic" euglenids (Triemer and Farmer 1991). The plastics (e.g. *Euglena*, *Peranema*, and *Distigma*) are either heterotrophic or phototrophic, are suspected to be monophyletic (Montegut-Felkner and Triemer 1997, Linton et al. 1999, Linton et al. 2000, Preisfeld et al. 2000), and have many pellicle strips (greater than 16) that are arranged helically and often permit the cell to undergo "euglenoid movement" (Gallo and Shrével 1982, Suzaki and Williamson 1985). The aplastics (e.g. *Petalomonas*, *Ploeotia*, and *Entosiphon*) are all heterotrophic, have a rigid pellicle of few longitudinally arranged strips (usually less than 12), and molecular data indicate that they may encompass the most recent common ancestor of euglenids (Triemer and Farmer 1991, Montegut-Felkner and Triemer 1997, Linton et al. 1999). Therefore, the aplastics may tag a paraphyletic group that, if made monophyletic within a strictly cladistic framework, would be synonymous with the Euglenida.

Comparative data from small subunit (SSU) rDNA indicate that some phototrophic taxa within the plastics have secondarily evolved a rigid pellicle (Linton et al. 1999, Linton et al. 2000). Traditionally, cells like these that were laterally flattened were classified as *Phacus* (Dujardin 1841) and those that were not flattened were placed into *Lepocinclis* (Perty 1849). Some members within these two taxa have acquired a pellicle with strips arranged longitudinally (e.g. *L. ovum* Lemmermann and *P. oscillans*), whereas others have retained helically arranged strips (e.g. *L. ovata* and *P. pyrum*). A close examination of whether pellicular features like rigidity, cell flatness, and strip orientation are homologous between members of *Lepocinclis* and *Phacus* has yet to take place. It is clear that the pellicle morphology within these taxa is very diverse, but how this diversity reflects phylogeny remains largely unexplored (Pochmann 1942, Huber-Pestalozzi 1955, Bourrelly and Couté 1981, Conforti and Tell 1983, 1989, Leedale 1985, Tell and Conforti 1986, Couté and Thérézien 1994, Zakrys and Walne 1994).

[1]Received 24 July 2000. Accepted 30 October 2000.

[2]Author for correspondence: e-mail bleander@arches.uga.edu.

One molecular analysis indicates that neither *Phacus* nor *Lepocinclis* are monophyletic and both are intermixed within *Euglena* Ehrenberg (Linton et al. 2000). Moreover, comparative analyses of other euglenids demonstrate that details of the pellicle provide important phylogenetic information (Buetow 1968, Leedale and Hibberd 1974, Cann 1986, Conforti and Tell 1989, Dragos et al. 1997, Angeler et al. 1999, Leander and Farmer 2000, 2001). We tested these hypotheses by providing data on the pellicle morphology of *Peranema trichophorum*, four *Phacus* taxa, one *Lepocinclis* taxon, and three *Euglena* taxa. Six of these taxa have rigid pellicles, and we suspect that they represent three separate clades that are not reflected in the current classification: (1) *L. ovata* and *P. pyrum*, (2) *E. tripteris* and *P. triqueter*, and (3) *P. oscillans* and *P. brachykentron*. The morphological data set was compared with previously published data for *Petalomonas cantuscygni*, *Distigma proteus*, *Entosiphon sulcatum*, and *Euglena gracilis*; analyzed cladistically; and coupled with comparative analyses of SSU rDNA sequences. We uncovered characters associated with the pellicle that provide robust apomorphy-based definitions for clades at different levels in the macroevolutionary hierarchy.

## MATERIALS AND METHODS

*Culture conditions.* Cultures of *Euglena acus* Ehrenberg (UTEX LB 1316), *E. stellata* (UTEX 372), *E. tripteris* (UTEX LB 1311), *Lepocinclis ovata* (UTEX LB 1305), *Phacus brachykentron* (UTEX LB 1317), *P. caudata* Hübner (UTEX LB 1285), *P. pyrum* (UTEX LB 2345), and *P. triqueter* (UTEX LB 1286) were obtained from the Culture Collection of Algae at the University of Texas at Austin (UTEX). *Euglena stellata* was grown in Proteose medium, and the remaining cultures were grown in a soil–water (GR+ / $NH_4$) medium (Starr and Zeikus 1993). All cultures were maintained in an incubator at 20° C and a 12:12 L:D cycle. Linton et al. (2000) contended that the culture of *P. caudata* was mislabeled and is actually *P. oscillans*. Because we examined cells from the same source, we also refer to this culture as *P. oscillans*. *Peranema trichophorum* was obtained from the Carolina Biological Supply Company (WW-13-1838). *Entosiphon sulcatum* was isolated from the Delaware–Raritan canal in New Brunswick, New Jersey, and a unialgal culture was temporarily maintained in soil–water medium that unfortunately is no longer available.

*Electron microscopy.* Cells from each culture were concentrated by slow centrifugation, chemically fixed, and prepared for transmission and scanning electron microscopy by the protocols described in Leander and Farmer (2000).

*Morphological descriptions and replicate observations.* The terminology used to describe pellicle morphology has been defined by Leander and Farmer (2000, 2001); terms dealing with strip substructure are reviewed in Table 1. To determine whether distinct surface patterns of strips were consistent within taxa, 30 different cells were scored and the mode and range of variation were presented.

*Phylogenetic analysis of morphological characters.* Nineteen pellicle characters containing 62 character states were scored for 13 euglenid taxa. The matrix of character states was analyzed with PAUP* 4.0 using the branch-and-bound algorithm (Swofford 1999). States for two characters were ordered, and the remainder was left unordered. The two ordered characters possess polar states that are linked by clear intermediate states (see Results). The robustness of each node on the most parsimonious tree(s) was investigated with decay indices using AutoDecay 4.0.2 (Eriksson 1998) and nonparametric bootstrap values using PAUP* 4.0. The tree length, number of informative characters, retention index, and consistency index were presented. Character state changes were phylogenetically mapped using MacClade 3.03.

*DNA isolation, amplification, and sequencing.* Genomic DNA was extracted from *E. tripteris*, *P. brachykentron*, and *P. triqueter* using a standard hexadecyltrimethylammonium bromide (CTAB) extraction protocol (Zolan and Pukkila 1986). After RNAse digestion, sequences of SSU rDNA were amplified using PCR primers and a thermocycling protocol established previously for the group (Elwood et al. 1985, Montegut-Felkner and Triemer 1997, Preisfeld et al. 2000). Three pairs of primers were used to amplify the genes in three fragments: 1AF, 5′ AAC CTG GTT GAT CCT GCC AGT 3′ and 516R, 5′ ACC AGA CTT GCC CTC C 3′; 300F, 5′ AGG GTT CGA TTC CGG AG 3′ and 1055R, 5′ CGG

TABLE 1. Terms used to describe the substructure of euglenid pellicle strips as preferred by Leander and Farmer (2001).

- **Arch:** The fraction of the frame between the overhang and the keel.
- **Articulation zone:** The space between the overhang of one strip and the hook of an adjacent strip. Bridges and microtubules are usually present within this zone.
- **Doublets:** A repeating unit of two strips that have different morphologies.
- **Frame:** The fundamental component of strips (i.e. the strip excluding lateral projections). The properties of frames are best demonstrated in transverse section. Usually, the frame is sigmoidal and consists of at least an overhang, an arch, a heel, and a hook.
- **Heel:** The fraction of the frame between the hook and the keel.
- **Hook:** The margin of a heel that resides below the overhang of an adjacent strip.
- **Keel:** A recognizable edge that defines the boundary between the arch and the heel.
- **Major groove:** The extracellular space formed between any two articulating strips. The properties of the heel of one strip and the overhang of an adjacent strip determine the properties of the groove (e.g. depth, shape, and width).
- **Median depression:** The concave surface on the arches of some taxa; associated with M-shaped strips.
- **Overhang:** The margin of an arch that resides above the hook of an adjacent strip.
- **Pellicle:** The cytoskeletal complex of euglenids consisting of the plasma membrane, proteinaceous strips, microtubules, and tubular cisternae of endoplasmic reticulum.
- **Postarticular projection:** Any proteinaceous extension branching off of the heel and positioned below the arch of the same strip. These projections often reside above the prearticular projections of an adjacent strip.
- **Prearticular projection:** Any proteinaceous extension branching off of the heel and positioned below the arch of an adjacent strip. These projections often reside below the postarticular projections of an adjacent strip.
- **Strip:** A repeating proteinaceous structure that lies directly below the plasma membrane and consists primarily of a frame that is often sigmoidal in transverse section. The strip also includes any strip projections that branch off of the heel laterally. Strips are arranged in parallel along the longitudinal axis of the cell and may have either a longitudinal or helical orientation.
- **Strip projections:** Proteinaceous structures that are continuous with the frame and branch laterally off of the heel. The projections may be either prearticular or postarticular depending on their position relative to the articulation zone.

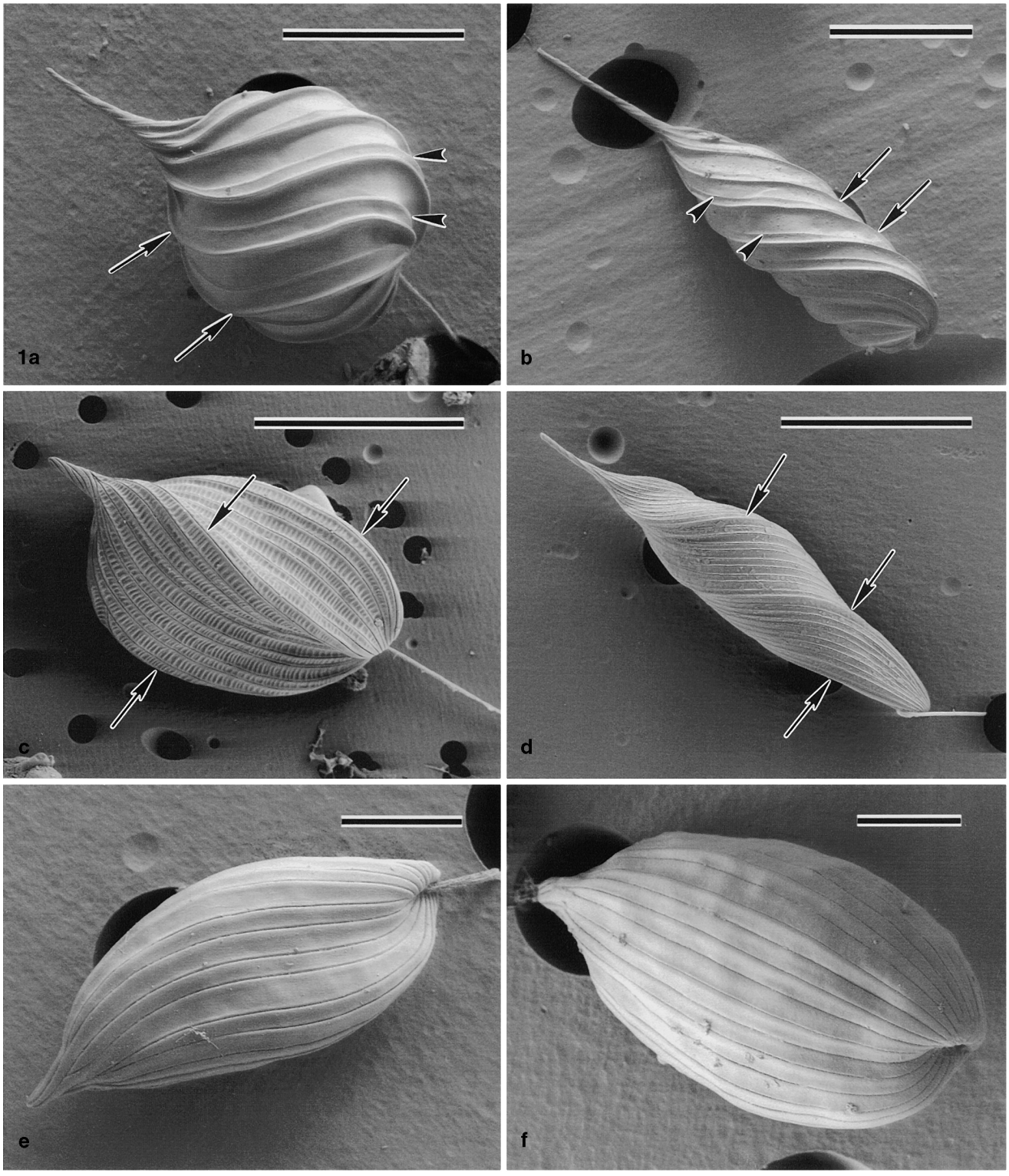


FIG. 1. Scanning electron micrographs illustrating the three major varieties of rigid pellicles present in taxa often classified as *Phacus*. (a) The helical pellicle of *Lepocinclis ovata* showing an alternating pattern of raised (arrows) and depressed (arrowheads) articulation zones. The posterior end is drawn out into a sharp "tail" (bar, 10 μm). (b) The helical pellicle of *Phacus pyrum* also consists of an alternating pattern of raised (arrows) and depressed (arrowheads) articulation zones plus a sharp posterior end (bar, 10 μm). (c) The helical pellicle of *Phacus triqueter* has three superridges (arrows) and a sharp posterior end (bar, 20 μm). (d) *Euglena tripteris* also has a helical pellicle with three superridges (arrows) (bar, 20 μm). (e) The pellicle of *Phacus oscillans* consists of longitudinally arranged strips and a short stubby posterior tip (bar, 5 μm). (f) The pellicle of *Phacus brachykentron* (bar, 5 μm).

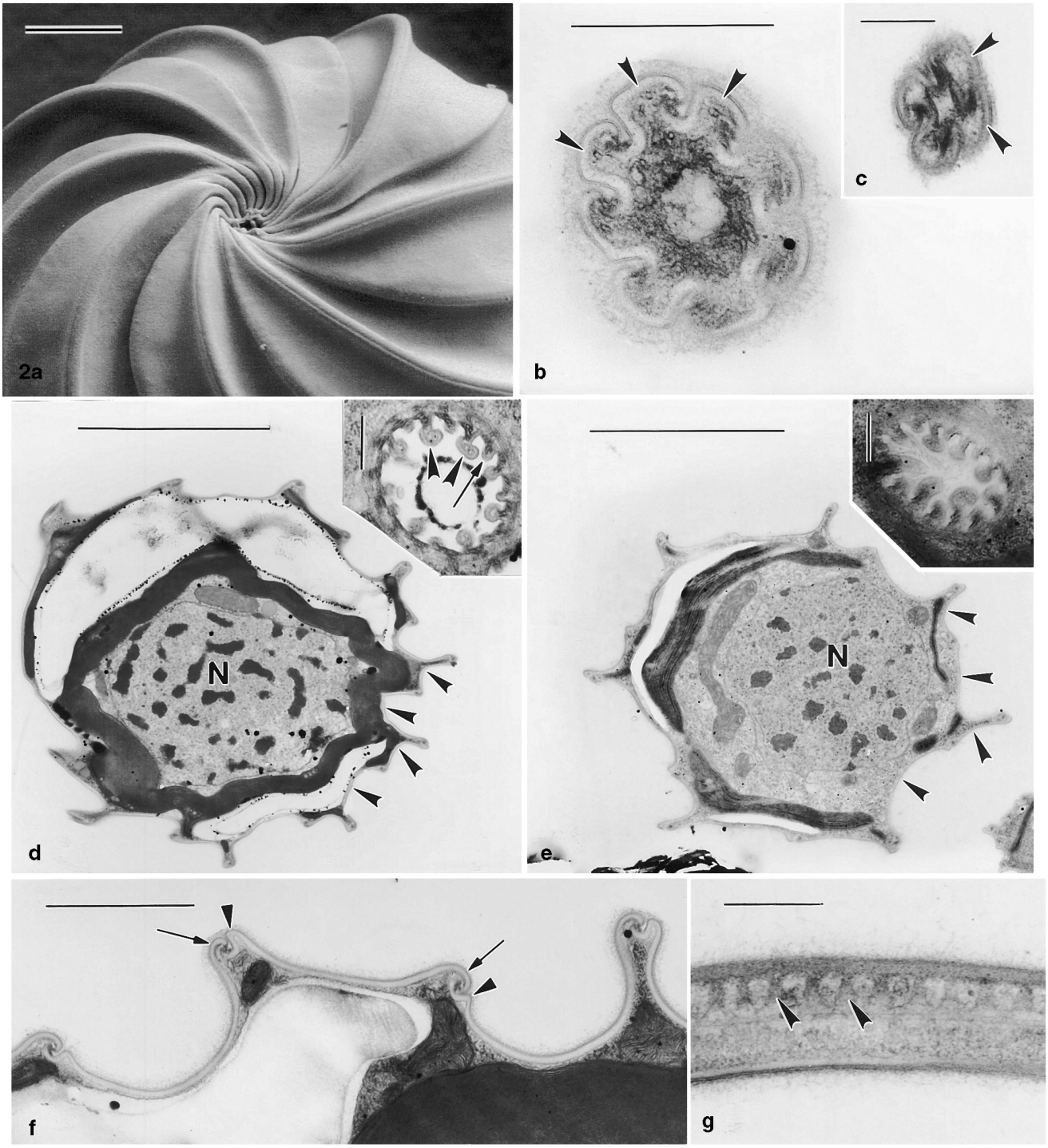


FIG. 2. Comparative morphology of *Lepocinclis ovata* and *Phacus pyrum*. (a) Scanning electron micrograph showing the anterior end of *L. ovata*. The broad peripheral strips dramatically decrease in width before entering the canal opening (bar, 2 μm). (b) Transverse transmission electron micrograph (TEM) showing the number of strips (arrowheads) that passed through the first whorl of strip reduction, whorl I, on the posterior tail of *L. ovata* (bar, 0.5 μm). (c) Transverse TEM showing the number of strips (arrowheads) that passed through the second whorl of strip reduction, whorl II, on the posterior tail of *L. ovata* (bar, 0.25 μm). (d) TEM at the level of the nucleus showing the transverse shape and the number of strips (arrowheads) around the periphery of *L. ovata* (bar, 5 μm). Inset: Transverse TEM through the canal of *L. ovata*. Although no strips terminate completely, every alternate strip (arrowheads) lining the canal is larger than the strips in between (arrow) (bar, 0.25 μm). (e) TEM at the level of the nucleus showing the transverse shape and the number of strips (arrowheads) around the periphery of *P. pyrum* (bar, 4 μm). Inset: Transverse TEM through the canal of *P. pyrum* (bar, 0.25 μm). (f) Transverse TEM through the strips of *L. ovata* showing M-shaped frames, keels (arrowheads), and overhangs (arrows). The arches are often more than 15 times the width of the heels. The doublets are based on an alternating pattern of raised and depressed articulation zones (bar, 1 μm). (g) Tangential TEM of *L. ovata* showing the "dovetailed" morphology of the prearticular projections (arrowheads) (bar, 0.25 μm).

CCA TGC ACC ACC 3′; 1055F, 5′ GGT GGT GCA TGG CCG 3′ and 1520B, 5′ TGA TCC TTC TGC AGG TTC ACC TAC 3′. The amplified DNA fragments were sequenced in both directions using the same primers and a Perkin-Elmer (Norwalk, CT) 310 Genetic Analyzer (capillary technology) following manufacturer's protocols. To cross-validate and optimize the nucleotides in the 5′–3′ sequence, the program Gene Runner 3.05 was used to align the complimentary sequences. Ambiguities and incongruities among the sequences from different primers were either resolved or scored as "uncertain" by interpreting the chromatographs.

*Alignment and phylogenetic analyses of sequence data.* The SSU rDNA sequences for *E. tripteris* (GenBank accesion AF286210), *P. brachykentron* (AF286209), and *P. triqueter* (AF286211) were compared with the previously published sequences for *Distigma proteus* (AF106036), *E. acus* (AF152104), *E. gracilis* (M12677), *E. stellata* (AF150936), *L. ovata* (AF061338), *Peranema trichophorum* (U84733, U84734), *Petalomonas cantuscigni* (U84731), *Phacus oscillans* (AF181968), and *P. pyrum* (AF112871).

Manual alignment was assisted by using the programs Clustal X 1.8 (Thompson et al. 1997) and Sequence Alignment Editor (Se-Al 1.0; Rambaut 1996). The alignment was improved using the SSU rDNA secondary structure of *E. gracilis*, *Peranema trichophorum*, and *Petalomonas cantuscygni* (Van de Peer et al. 1999, Linton et al. 2000); the final alignment is available from the authors on request. A total of 1303 base positions was unambiguously aligned and used for parsimony and maximum likelihood analyses. Nucleotides and gaps were treated as independent unordered character states of equal weight. PAUP* 4.0 was used to run the branch-and-bound algorithm with ACCTRAN character state optimization, tree bisection-reconnection branch swapping, random stepwise addition of taxa, and MULTREES on. Decay indices were generated with AutoDecay 4.0.2 (Eriksson 1998) to evaluate the robustness of each node on the parsimony tree. Even though the sample size was small, nonparametric bootstrap values were generated using PAUP* 4.0 (Felsenstein 1985). The tree length, number of informative characters, consistency index, and retention index were reported.

The topology of the parsimony tree was compared with a tree derived from a maximum likelihood algorithm on PAUP* 4.0. Maximum likelihood analyses were performed using empirical nucleotide frequencies and two substitution types corresponding with the Hasegawa-Kishino-Yano model. A molecular clock was not enforced, tree bisection-reconnection branch swapping was used, and starting branch lengths were obtained using the Rogers-Swofford approximation method. To estimate how well the data supported each node on the maximum likelihood tree, 10 replications with random addition of taxa were performed for each of 100 bootstrap replicates.

*Outgroup justification.* The euglenid *Petalomonas cantuscygni* was chosen as the outgroup for both the morphological and the molecular analyses. Previous phylogenetic analyses of molecular data demonstrate that this taxon is the sister taxon to all other euglenids with a known SSU rDNA sequence (Montegut-Felkner and Triemer 1997, Linton et al. 1999, Preisfeld et al. 2000). Also, comparative analyses of morphology indicate that the pellicle of *Petalomonas* includes many ancestral states, such as cell rigidity and few strips (more than eight) that are broad, fused, and longitudinally arranged (Farmer 1988, Montegut-Felkner and Triemer 1997, Leander and Farmer, 2001).

## RESULTS

### *Comparative morphology of the pellicle*

*The pellicle of* Lepocinclis ovata *and* Phacus pyrum. At least three major varieties of rigid pellicles are found within taxa classified as *Phacus* (Fig. 1, a–f). These pellicle varieties are also found in taxa other than *Phacus*. For instance, one variety is present in both *Phacus pyrum* and *Lepocinclis ovata* (Figs. 1, a and b, and 2, a–g). The basic strip substructure for *P. pyrum* has been described previously (Leander and Farmer 2001). Like *P. pyrum*, the frames of *L. ovata* were M shaped. The strips were arranged as doublets that produced an alternating pattern of raised and depressed articulation zones (Figs. 1a and 2f). One strip within each doublet possessed a keel associated with a raised articulation zone and an arch associated with a depressed articulation zone, whereas the companion strip took on the opposite configuration (Figs. 1a and 2f). In both taxa, the arches were very broad near the midsection of the cell and were often more than 15 times wider than the heels (Figs. 1a and 2f). As the strips approached the anterior and posterior ends of the cell, the median depression within each arch disappeared. Also, the arches became much narrower until reaching a width that approximated the width of the heels (Fig. 2, a and b). The preartícular projections were novel in that

TABLE 2. The number of strips reduced on each whorl present in the investigated euglenids.

| | Taxon | | | | | | | |
|---|---|---|---|---|---|---|---|---|
| Character | *Phacus oscillans*[a] (22 / 30) P = 20 (16–22) | *Phacus brachykentron*[b] (30 / 30) P = 32 | *Euglena acus* (19 / 30) P = 28 (28–36) | *Euglena tripteris* (30 / 30) P = 32 | *Phacus triqueter* (30 / 30) P = 32 | *Phacus pyrum* (27 / 30) P = 16 (14–19) | *Lepocinclis ovata* (27 / 30) P = 16 (12–20) | *Euglena stellata* (27 / 30) P = 40 (36–44) |
| Anterior whorls | | | | | | | | |
| *i* | 20–10 | 32–16 | 28–14 | 32–16 | 32–16 | — | — | 40–20 |
| Posterior whorls | | | | | | | | |
| I | 20–9[c] | 32–16 | 28–14 | 32–16 | 32–16 | 16–8 | 16–8 | 40–20 |
| II | — | 16–8[d] | 14–7 | 16–8 | 16–8 | 8–4 | 8–4 | 20–10 |
| III | — | — | — | 8–4 | 8–4 | — | — | — |

"P" refers to the number of strips around the periphery; the range of variation is shown parenthetically below the mode. The frequency of the mode for P over the number of cells observed is positioned directly below each taxon. For each pair of numbers associated with the anterior and posterior whorls, the first refers to the number of strips entering a particular whorl and the second is the number of strips that continue through the whorl.

[a] Pseudoexponential pattern of strip reduction at posterior end.

[b] Clustered pattern of strip reduction at posterior end.

[c] The whorl in which the exponential pattern breaks down.

[d] The whorl on which two identical clusters of four terminating strips are positioned equidistantly.

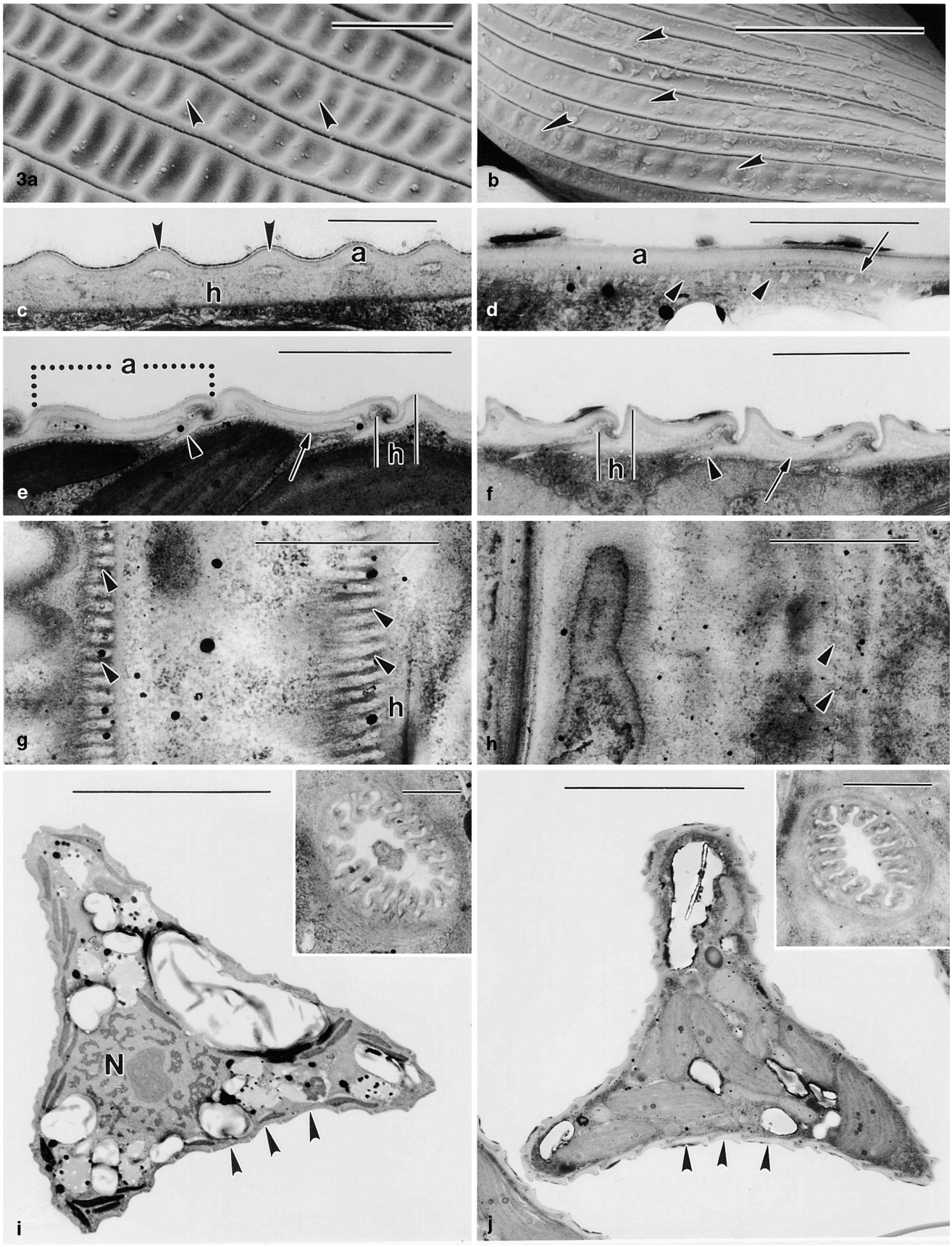
3a
b
a
h
c
a
d
a
h
e
h
f
h
g
h
N
i
j

they had a structure that may be described as "dovetailed" (Fig. 2g). Postarticular projections were not observed in either taxon.

The cell shape of both *L. ovata* and *P. pyrum* was round in transverse section (Fig. 2, d and e). The cell shape in longitudinal section was round in *L. ovata* and fusiform in *P. pyrum*. The maximum number of strips around the cell periphery (P) had a mode of 16 in both taxa (Fig. 2, d and e, and Table 2). The strips were arranged helically and oriented clockwise when viewed from the anterior end (Fig. 1, a and b). Every strip around the cell periphery entered a canal opening that was positioned apically (Fig. 2a). There was no clear whorl of strip reduction within the canal (i.e. $W_A = 0$), although every alternate strip was larger than the strips in between (insets in Fig. 2, d and e, and Table 2). The larger strips lining the canal had a distinctive "paddle shape" in transverse section (insets in Fig. 2, d and e). The posterior end of both taxa was drawn out into a very sharp "tail" (Fig. 1, a and b). At the posterior end, the 16 peripheral strips decreased exponentially across two whorls (i.e. $W_P = 2$) (Fig. 2, b and c, and Table 2).

*The pellicle of* Euglena tripteris *and* Phacus triqueter. A second major variety of rigid pellicle is present in *Phacus triqueter* and *Euglena tripteris* (Figs. 1, c and d, 3a, and 4b). The arches possessed "struts" (Leedale 1985) that were positioned perpendicular to the longitudinal axis of the strips (Figs. 1c and 3, a–c). In *P. triqueter*, the struts were robust, evenly spaced, and present on every strip (Fig. 3, a and c). By contrast, in *E. tripteris*, the struts were less robust and present only on every alternate strip (Fig. 3b). The frames in both taxa were M shaped and consisted of a keel separating an arch that was over five times the width of the heel (Fig. 3, e and f). The keels of *E. tripteris* were significantly sharper than the keels of *P. triqueter* (Fig. 3, e and f). The short prearticular projections of both taxa were teethlike and approximately equal in width to the heels (Fig. 3, d–h). The postarticular projections formed indented plates that extended beneath most of the arch (Fig. 3, d–h). Compared with *P. triqueter*, the postarticular projections of *E. tripteris* were shorter relative to the arch and thicker near the heel (Fig. 3, e and f).

Both *P. triqueter* and *E. tripteris* possessed rigid pellicles with three superridges, giving cells a deltoid shape when viewed in transverse section (Figs. 1, c and d, and 3, i and j). The shape of the cells in longitudinal section was ovoid in *P. triqueter* and fusiform in *E. tripteris*. The strips were arranged helically; however, in *P. triqueter* they were oriented clockwise when viewed from the anterior end and in *E. tripteris* they were counterclockwise (Fig. 1, c and d). For both taxa, P = 32 (Fig. 3, i and j, and Table 2). All strips entered the canal opening and reduced exponentially across one whorl at the anterior end (i.e. $W_A = 1$); 16 strips lined the canal (insets in Fig. 3, i and j, and Table 2). Like *P. pyrum* and *L. ovata*, the posterior end is drawn out into a sharp tail (Fig. 1, c and d). In both *P. triqueter* and *E. tripteris*, the strips reduced exponentially across three whorls at the posterior end (i.e. $W_P = 3$) (Fig. 4, a and b, and Table 2). The posterior whorls of strip termination on *E. tripteris* were obvious and evenly spaced (Fig. 4b). By contrast, the posterior end of *P. triqueter* appeared to have been compressed and twisted, making the posterior whorls more difficult to score (Fig. 4a). For example, near each of the three superridges, one terminating strip from whorl I was positioned very close to one terminating strip from whorl II (Fig. 4a, arrows). This contributed in making whorls I and II irregular. Because we knew that P = 32, T = 4 (where T is the number of strips that converge at the posterior tip) and S = 1 (where S is the number of strips between two consecutively terminating strips), the equation for exponential strip reduction, $W_P = 1/k \cdot \ln (T/P)$, given by Leander and Farmer (2000), helped us confirm that $W_P = 3$ in *P. triqueter*; the exponential rate constant "k" is equivalent to ln (0.5) when S = 1 (Leander and Farmer 2000).

*The pellicle of* Phacus brachykentron *and* P. oscillans. *Phacus brachykentron* and *P. oscillans* possess a third major variety of rigid pellicle, where the strips are arranged longitudinally (Fig. 1, e and f). The cells were ovoid in both longitudinal and transverse section (Figs. 1, e and

FIG. 3. Comparative morphology of *Phacus triqueter* and *Euglena tripteris*. (a) Scanning electron micrograph of *P. triqueter* showing struts (arrowheads) oriented perpendicular to the longitudinal axis of the strips (bar, 2 μm). (b) Scanning electron micrograph of *E. tripteris* showing struts (arrowheads) oriented perpendicular to the longitudinal axis of the strips. Struts only occur on every alternate strip (bar, 5 μm). (c) Longitudinal transmission electron micrograph (TEM) of *P. triqueter* showing that the struts (arrowheads) are ripples in the arches (a). This section passed through the heel (h) of the same strip (bar, 0.5 μm). (d) Longitudinal TEM of *E. tripteris* showing teethlike prearticular projections (arrowheads) subtending the postarticular projections, which form an indented plate (arrow). The postarticular projections, in turn, subtend the arch (a) (bar, 0.5 μm). (e) Transverse TEM of *P. triqueter* showing short prearticular projections (arrowhead) and long postarticular projections (arrows) branching from the heel (h). The arch (a) is approximately five times the width of the heel (bar, 1 μm). (f) Transverse TEM of *E. tripteris* showing short prearticular projections (arrowhead) and postarticular projections (arrows) with thick bases fixed to the heel (h). The arch (a) is approximately five times the width of the heel (bar, 0.5 μm). (g) Tangential TEM of *P. triqueter* at the level of the teethlike prearticular projections (arrowheads), which attach to the heel (h) (bar, 1 μm). (h) Tangential TEM of *E. tripteris* at the level of the postarticular projections, which form an indented plate (the fine horizontal striations). Teethlike prearticular projections (arrowheads) are also visible (bar, 0.5 μm). (i) Transverse TEM of *P. triqueter* at the level of the nucleus showing the deltoid transverse shape of the cell and the number of strips (arrowheads) around the periphery (bar, 10 μm). Inset: Transverse TEM showing that only half the number of strips around the periphery line the canal (bar, 0.5 μm). (j) Transverse TEM of *E. tripteris* at level posterior to the nucleus showing the deltoid transverse shape of the cell and the number of strips (arrowheads) around the periphery (bar, 3 μm). Inset: Transverse TEM showing that only half the number of strips around the periphery line the canal (bar, 0.5 μm).

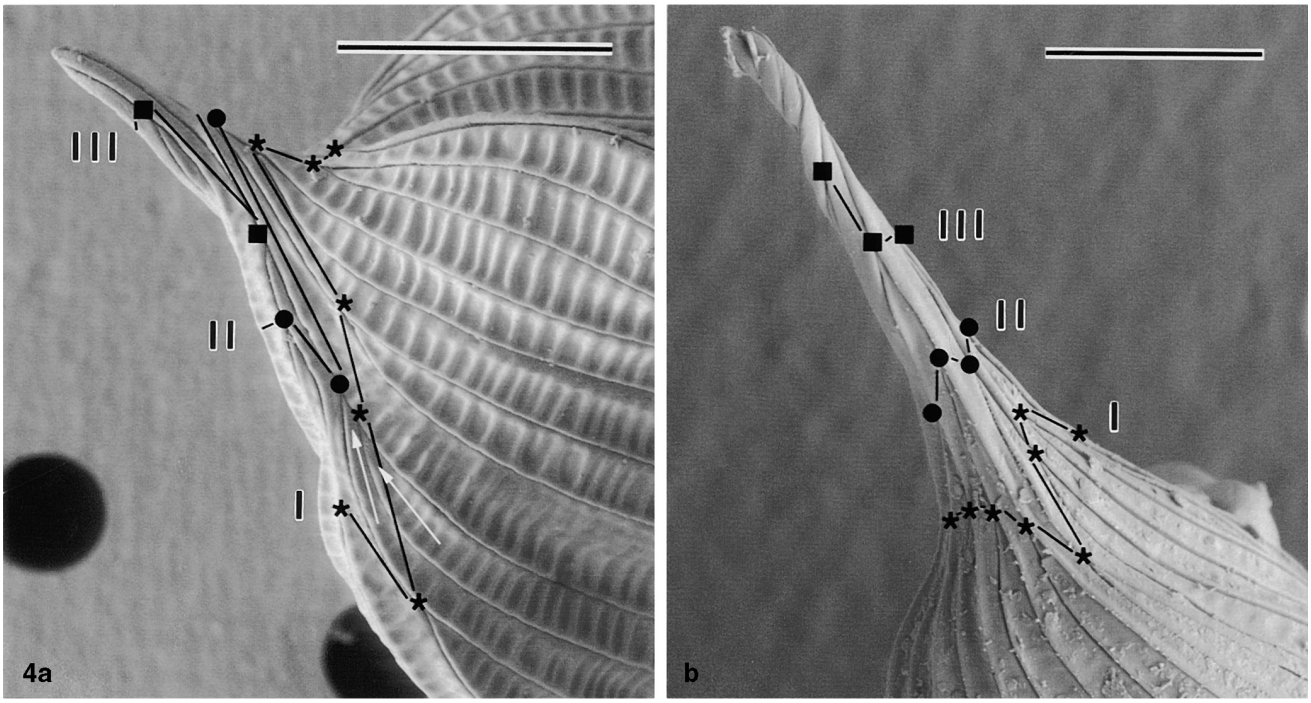


FIG. 4. The whorls of strip reduction at the posterior end of *Phacus triqueter* and *Euglena tripteris*. (a) Scanning electron micrograph of *P. triqueter* showing an exponential pattern of strip reduction consisting of three whorls. Every alternate peripheral strip terminates on whorl I (asterisks). Every alternate strip that passed through whorl I terminates on whorl II (circles). Every alternate strip that passed through whorl II terminates on whorl III (squares). Near every superridge a terminating strip on whorl I is positioned very close to a terminating strip on whorl II (arrows). This suggests that the posterior end was compressed and twisted resulting in whorls that are irregularly shaped and crowded rather than circular and evenly spaced. (bar, 2.5 μm). (b) Scanning electron micrograph of *E. tripteris* showing an exponential pattern of strip reduction consisting of three evenly spaced whorls. Every alternate peripheral strip terminates across whorl I (asterisks). Every alternate strip that passed through whorl I terminates on whorl II (circles). Every alternate strip that passed through whorl II terminates on whorl III (squares) (bar, 1.25 μm).

f, and 5, a and b). In *P. oscillans* and *P. brachykentron*, a subtle longitudinal cleft extended from a canal opening that was positioned subapically. In *P. brachykentron*, P = 32 in all cells observed; in *P. oscillans*, the mode P was 20 and the range was 16–22 (Fig. 5, a and b, and Table 2). In both taxa, the strips reduced exponentially across a single whorl near the canal opening, resulting in half of the peripheral strips lining the canal (i.e. $W_A = 1$) (insets in Fig. 5, a and b). The posterior end of these taxa consisted of a short stubby tip. The strips reduced pseudoexponentially (no complete halving event occurs; e.g. 20 strips reduce to 9) across a single whorl near the posterior end of *P. oscillans* (i.e. $W_P = 1$) (Fig. 5f and Table 2). In quantitative terms, the strips reduced exponentially across two whorls at the posterior end of *P. brachykentron* (i.e. $W_P = 2$) (Fig. 5g and Table 2). However, the inner whorl was novel in that there were two symmetrically positioned clusters of

FIG. 5. Comparative morphology of *Phacus oscillans* and *P. brachykentron*. (a) Transverse transmission electron micrograph (TEM) of *P. oscillans* at the level of the nucleus showing the number of strips around the periphery (arrowheads) and the ovoid transverse shape of the cell (bar, 3 μm). Inset: Transverse TEM showing that half the number of peripheral strips line the canal (bar, 0.25 μm). (b) Transverse TEM of *P. brachykentron* at the level of the nucleus showing the number of strips around the periphery (arrowheads) and the ovoid transverse shape of the cell (bar, 6 μm). Inset: Transverse TEM showing that half the number of peripheral strips line the canal (bar, 0.5 μm). (c) Transverse TEM through the strips of *P. oscillans* showing prearticular projections (arrowhead), postarticular projections (arrows), and arches that are more than three times the width of the heels (bar, 0.5 μm). (d) Tangential TEM of *P. oscillans* at the level of the articulation zones (az) and teethlike prearticular projections (arrowheads) (bar, μm). (e) Tangential TEM of *P. oscillans* at the level of an articulation zone (az) and postarticular projections, which form an indented plate (fine vertically oriented striations) (bar, 0.5 μm). (f) Scanning electron micrograph of *P. oscillans* showing that the peripheral strips reduce pseudoexponentially across a single whorl (I) near the posterior end. Every alternate peripheral strip (asterisks) plus one additional strip (arrow) terminate on whorl I (bar, 0.5 μm). (g) Scanning electron micrograph of *P. brachykentron* showing the pattern of terminating strips at the posterior end. Every alternate peripheral strip (asterisks) terminates on whorl I. Half of the strips that passed through whorl I terminate in two symmetrically positioned clusters (arrows). Each cluster consists of three consecutive strips (1, 2, and 3) that terminate on the lateral margin of a fourth strip (4) that, in turn, terminates nearer but short of the posterior tip. Nine peripheral strips reside between the fist strip of one cluster and the fourth strip of the other cluster (bar, 1 μm).

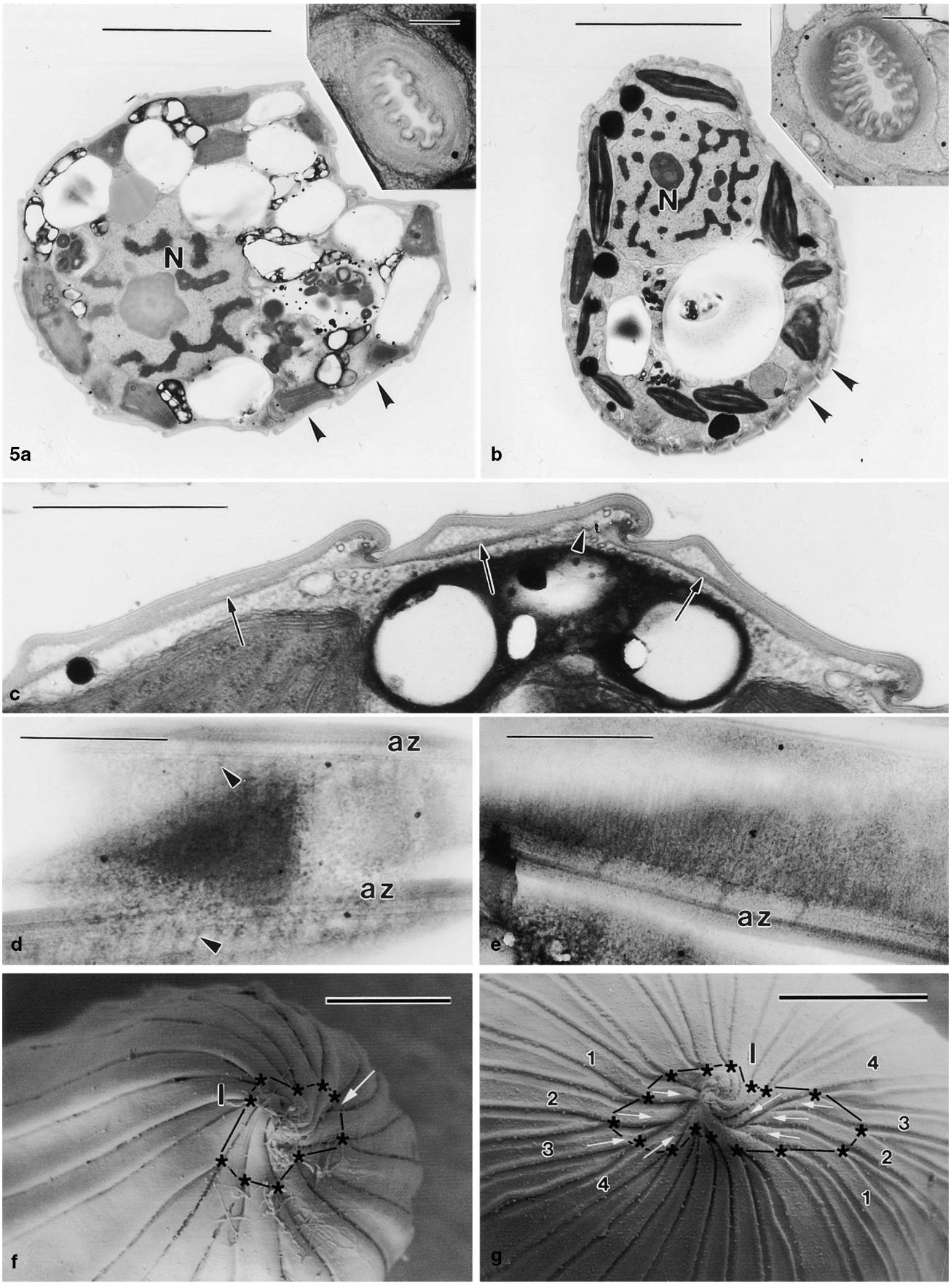
N
5a
N
b
c
az
az
d
az
e
l
f
1
l
4
2
3
3
2
4
1
g

TABLE 3. Morphological characters and states associated with the pellicle of the 13 taxa included in the phylogenetic analysis.

| Character | State |
|---|---|
| 1) Orientation of strips | 0, longitudinal; 1, helical; 2, semilongitudinal; 3, longitudinal with a posterior twist |
| 2) Handedness of helix[a] | 0, CCW; 1, CW |
| 3) Strips lining the canal | 0, no; 1, yes |
| 4) P[b] | 0, 8–12; 1, 16; 2, 18–20; 3, 28–32; 4, 36–40; 5, 50–54 |
| 5) $W_A$ | 0, 0; 1, 1 |
| 6) $W_P$ | 0, 0; 1, partial[c]; 2, 1; 3, 2; 4, 3 |
| 7) Clustered reduction | 0, no; 1, yes |
| 8) Pellicle pores | 0, absent; 1, present |
| 9) Pellicle plasticity | 0, rigid; 1, plastic; 2, semiplastic |
| 10) Transverse shape of cell | 0, ovoid; 1, circular; 2, deltoid |
| 11) Morphology of posterior end | 0, keeled; 1, rounded; 2, oblique; 3, conical; 4, sharp; 5, stubby |
| 12) Overhang | 0, no; 1, yes |
| 13) Struts on arches | 0, no; 1, yes |
| 14) Shape of frames | 0, U-shaped; 1, S-shaped; 2, plateau; 3, M-shaped; 4, robust[d] |
| 15) Keel | 0, no; 1, yes |
| 16) Widths of arch and heel | 0, heel > 3× arch; 1, arch ≈ heel; 2, arch ≈ 2× heel; 3, arch > 3× heel; 4, arch > 10× heel |
| 17) Prearticular projections | 0, absent; 1, threadlike; 2, teethlike; 3, dovetailed |
| 18) Postarticular projections | 0, absent; 1, threadlike; 2, indented plate; 3, teethlike |
| 19) Doublet identity | 0, none; 1, heels, 2, articulation zones |

Symbols for the characters and character states used in Table 4 are shown.

[a] Viewed from the anterior end.

[b] Mode from 30 cells scored.

[c] Strips at the posterior end converge on a common line; most of the strips (e.g. 42 of 52) terminate on one side of the line and show an alternate pattern of strip reduction.

[d] Thick frames with a subtle median depression in the arch.

CCW = counterclockwise; CW = clockwise.

terminating strips rather than the usual alternating pattern of terminating strips (Fig. 5g, arrows). Both clusters consisted of three consecutive strips terminating onto the lateral margin of a fourth strip that, in turn, terminated nearer but short of the posterior end. Nine peripheral strips were positioned between the first strip of one cluster and the fourth strip of the other cluster (Fig. 5g). This same pattern was present on all ten *P. brachykentron* cells observed.

The basic strip substructure for *P. brachykentron* has been described previously (Leander and Farmer 2001). Like *P. brachykentron*, the frames of *P. oscillans* are robust with a slight median depression (Fig. 5c). A keel is present and the arches are more than three times the width of the heels (Fig. 5c). The prearticular and postarticular projections of *P. oscillans* were similar to those in *P. triqueter* and *E. tripteris*. The prearticular projections are teethlike and about equal in width to the heel; the postarticular projections form indented plates that extend below most of the arch (Fig. 5, c–e). The postarticular projections of *P. brachykentron* did not form an indented plate but were teethlike (Leander and Farmer 2001).

*The pellicle of* Euglena acus *and* E. stellata. For comparative purposes, we also examined the pellicles, particularly surface patterns, of two other phototrophic taxa: *Euglena acus* and *E. stellata*. The strip substructure *E. acus* has been examined previously (Mignot 1965, Bricheux and Brugerolle 1986) and consists of the same frame structure found in *P. brachykentron* and *P. oscillians*. Also like these *Phacus* taxa, the strips of *E. acus* are arranged longitudinally in relaxed cells. In contrast, *E. acus* was capable of a slight degree of euglenoid movement where the strips become helically arranged and oriented counterclockwise. The mode for P = 28, where the strips reduced exponentially across a single whorl at the anterior end (i.e. $W_A = 1$) and across two whorls at the posterior end (i.e. $W_P = 2$). Like in *L. ovata*, *P. pyrum*, *P. tripteris*, and *P. triqueter*, the posterior end of *E. acus* extended into a sharp tail.

*Euglena stellata* possessed a nonrigid pellicle that was very similar to *E. gracilis*, a pellicle that has been studied extensively (Kirk and Juniper 1964, Schwelitz et al. 1970, Lefort-Tran et al. 1980, Dubreuil and Bouck 1985, Leander and Farmer 2000). Both of these taxa possess strips that are arranged helically in a clockwise direction and permit the cell to undergo euglenoid movement. The cells were round in transverse section and fusiform in longitudinal section. A mode of 40 strips surrounded the periphery, P = 40, and reduced to 20 across a single whorl near the canal opening, $W_A = 1$ (Table 2). In *E. stellata*, the posterior end tapered into a conical tip and the strips around the periphery were reduced exponentially across two whorls (i.e. $W_P = 2$) (Table 2). Four to eight strips were positioned between rows of pellicle pores on the surface of *E. stellata*. In both taxa, the frames were plateau shaped, keels were present, and the arches were approximately twice the width of the heels. The prearticular projections were threadlike in both taxa. By contrast to the threadlike postarticular projections of *E. gracilis*, *E. stellata* possessed very fine indented plates.

*The pellicle of* Peranema trichophorum. We also examined the pellicle of *Peranema trichophorum* but report only the information necessary for the focused analysis in this article. The number of strips around the cell periphery was 50–54 in 10 cells, where the mode was 52. The strips were arranged helically and oriented in a

TABLE 4. Matrix of 19 morphological characters for 13 taxa used in the parsimony analysis to infer phylogenetic relationships.

| | Character | | | | | | | | | | | | | | | | | | |
|---|---|---|---|---|---|---|---|---|---|---|---|---|---|---|---|---|---|---|---|
| Character Style | R | U | U | U | U | R | U | U | U | U | U | U | U | U | U | U | U | U | U |
| | | | | | | | | | | 1 | 1 | 1 | 1 | 1 | 1 | 1 | 1 | 1 | 1 |
| Taxon | 1 | 2 | 3 | 4 | 5 | 6 | 7 | 8 | 9 | 0 | 1 | 2 | 3 | 4 | 5 | 6 | 7 | 8 | 9 |
| *Petalomonas cantuscygni* | 0 | – | 0 | 0 | – | 0 | 0 | 0 | 0 | 0 | 0 | 0 | 0 | 0 | 0 | 0 | 0 | 0 | 0 |
| *Entosiphon sulcatum* | 0 | – | 0 | 0 | – | 0 | 0 | 0 | 0 | 0 | 1 | 0 | 0 | 1 | 0 | 1 | 0 | 0 | 1 |
| *Distigma proteus* | 1 | 0 | 0 | 2 | – | 0 | 0 | 0 | 1 | 1 | 1 | 1 | 0 | 1 | 0 | 1 | 0 | 0 | 0 |
| *Peranema trichophorum* | 1 | 0 | 1 | 5 | N | 1 | 0 | 0 | 1 | 1 | 2 | 1 | 0 | 1 | 0 | 1 | 0 | 0 | 0 |
| *Euglena gracilis* | 1 | 0 | 1 | 4 | 1 | 4 | 0 | 1 | 1 | 1 | 1 | 1 | 0 | 2 | 1 | 2 | 1 | 1 | 0 |
| *Euglena stellata* | 1 | 0 | 1 | 3 | 1 | 4 | 0 | 1 | 1 | 1 | 3 | 1 | 0 | 2 | 1 | 2 | 1 | 2 | 0 |
| *Euglena tripteris* | 1 | 0 | 1 | 3 | 1 | 4 | 0 | 0 | 2 | 2 | 4 | 1 | 1 | 3 | 1 | 3 | 2 | 2 | 0 |
| *Phacus triqueter* | 1 | 1 | 1 | 3 | 1 | 4 | 0 | 0 | 0 | 2 | 4 | 1 | 1 | 3 | 1 | 3 | 2 | 2 | 0 |
| *Lepocinclis ovata* | 1 | 0 | 1 | 1 | 0 | 3 | 0 | 0 | 0 | 1 | 4 | 1 | 0 | 3 | 1 | 4 | 3 | 0 | 2 |
| *Phacus pyrum* | 1 | 0 | 1 | 1 | 0 | 3 | 0 | 0 | 0 | 1 | 4 | 1 | 0 | 3 | 1 | 4 | 3 | 0 | 2 |
| *Euglena acus* | 2 | 0 | 1 | 3 | 1 | 3 | 0 | 0 | 2 | 1 | 4 | 1 | 0 | 4 | 1 | 3 | 2 | 2 | 0 |
| *Phacus brachykentron* | 3 | – | 1 | 3 | 1 | 3 | 1 | 0 | 0 | 0 | 5 | 1 | 0 | 4 | 1 | 3 | 2 | 3 | 0 |
| *Phacus oscillans* | 3 | – | 1 | 2 | 1 | 2 | 0 | 0 | 0 | 0 | 5 | 1 | 0 | 4 | 1 | 3 | 2 | 2 | 0 |

Character styles are as follows: U, unordered character states; R, ordered character states. The symbols for the characters and character states are defined in Table 3. N, unknown.

counterclockwise direction as viewed from the anterior end. The pattern of strip reduction near the posterior end was novel and will be described more comprehensively in a future contribution. For our purposes, it is important to note that strip reduction did occur near the posterior end, and the strips converged on a common line rather than a common point as observed in all other taxa examined so far (Leander and Farmer 2000). An alternating pattern of strip reduction occurred only on one side of this line, the side where most of the strips (e.g. 42 of 52) terminated (data not shown); thus, we describe this state as "partial" strip reduction rather than a "whorl" of strip reduction.

*Phylogenetic analysis of pellicle characters.* The morphological character states described above are organized in Table 3. The data matrix used in the phylogenetic analysis is shown in Table 4. We ordered the states for 2 of the 19 characters, namely characters 1, orientation of strips, and 6, $W_P$ (Tables 3 and 4). From an evolutionary perspective, it was reasonable to require that helical pellicles and longitudinal pellicles with a twisted posterior end were linked by a semi-longitudinal pellicle, where the strips are arranged longitudinally in the relaxed stage and helically in contracted stages (e.g. *E. acus*) (character 1). In addition, the states for $W_P$ (character 6) were ordered because it made sense biologically that $W_P = 1$ and $W_P = 3$ was bridged by $W_P = 2$.

Figure 6 shows the strict consensus tree for three most parsimonious trees derived from the branch-and-bound algorithm. There were four least inclusive clades, each consisting of two taxa: (1) *E. gracilis* and *E. stellata*, (2) *L. ovata* and *P. pyrum*, (3) *E. tripteris* and *P. triqueter*, and (4) *P. brachykentron* and *P. oscillans*. *Euglena acus* grouped with the clade consisting of *P. brachykentron* and *P. oscillans*. The taxa between *L. ovata* through *P. oscillans* formed a more inclusive clade that contained a trichotomy at the ancestral node and was the sister to the clade consisting of *E. gracilis* and *E. stellata*. All the phototrophic taxa (*E. gracilis* through *P. oscillans*) comprised a single clade that diverged after the lineages, leading to *Peranema trichophorum* and *Distigma proteus*, which are both colorless. The tree indicated that *Peranema trichophorum* is more closely related to the phototrophs than to *Distigma proteus*.

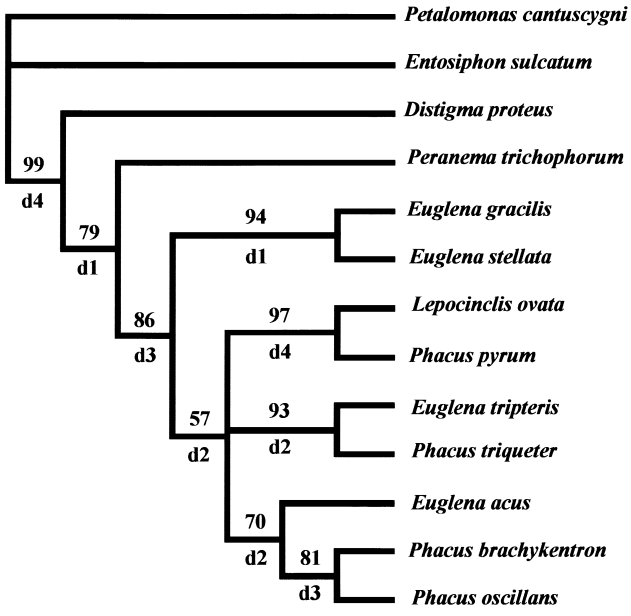


FIG. 6. Strict consensus tree of three most parsimonious trees using branch-and-bound on the data matrix derived from euglenid pellicle morphology (Table 4). The number above each stem are bootstrap values from 100 replications; the symbols below each stem represent decay indices.

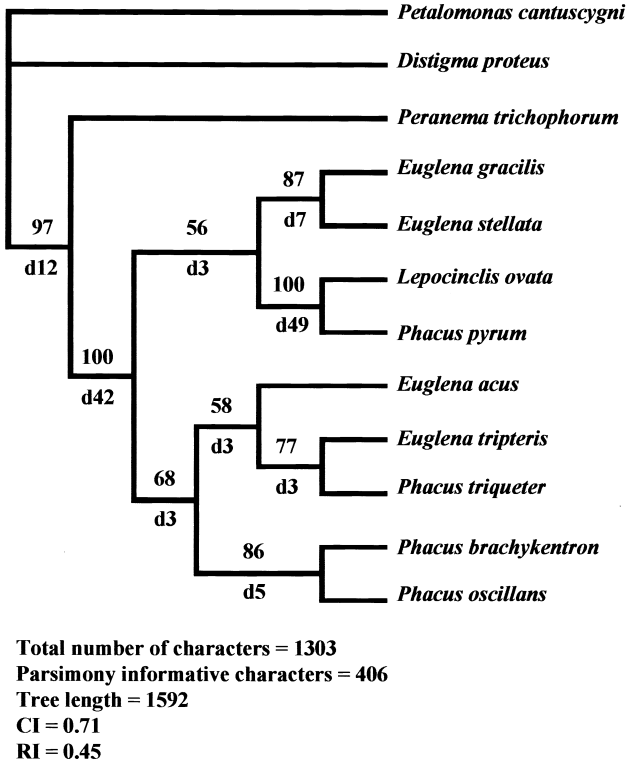


FIG. 7. The single most parsimonious tree using branch-and-bound on aligned SSU rDNA sequences from 12 euglenid taxa. The number above each stem represent bootstrap values and the symbols below are decay indices.

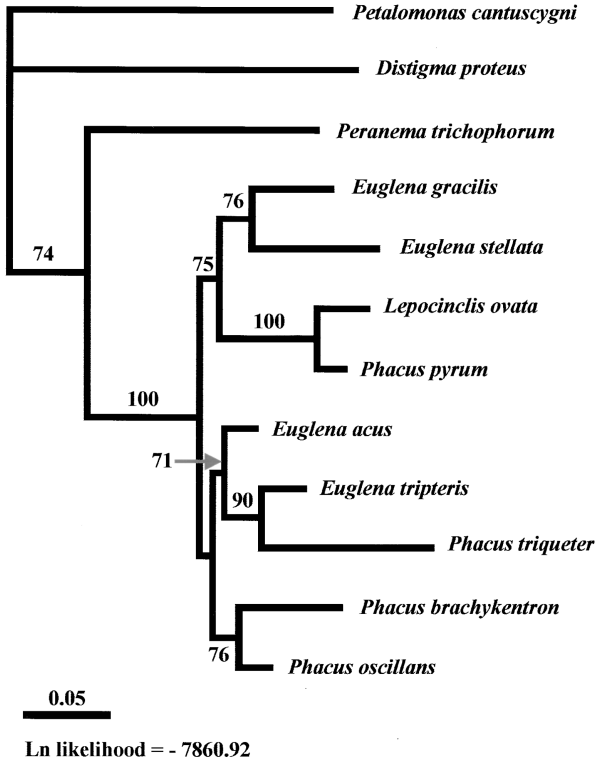


FIG. 8. Phylogram using maximum likelihood on aligned SSU rDNA sequences from 12 euglenid taxa. The numbers above each stem represent bootstrap percentages from 100 replications.

*Phylogenetic analysis of SSU rDNA.* The branch-and-bound and maximum likelihood analyses produced trees with identical topologies (Figs. 7 and 8). These sequence comparisons demonstrated the same four least inclusive clades found in the parsimony analysis of pellicle characters. The *L. ovata–P. pyrum* clade and the *E. gracilis–E. stellata* clade were sister groups and together formed a more inclusive clade that was only weakly supported (bootstrap = 56% with parsimony) in the branch-and-bound analysis. The analyses also suggested with weak bootstrap support (bootstrap = 58% with parsimony) that *E. acus* was the sister group to the *E. tripteris–P. triqueter* clade, and these three taxa formed a more inclusive clade with *P. brachykentron* and *P. oscillans*. Like in the tree derived from pellicle morphology, the phototrophic taxa formed a clade that was the sister group to *Peranema trichophorum*.

## DISCUSSION

*Comparative topology of the phylogenetic trees.* A comparison of the tree topologies derived from pellicle morphology and SSU rDNA demonstrates a high degree of concordance (Fig. 9). Two nodes, however, are incongruent between the two data sets, namely the precise phylogenetic positions of *E. acus* and the *L. ovata–P. pyrum* clade. Even though *E. acus* emerges as the sister to either the *P. brachykentron–P. oscillans* clade (pellicle morphology data set) or the *E. tripteris–P. triqueter* clade (SSU rDNA data set), these five taxa always group together in the next more inclusive clade. The *L. ovata–P. pyrum* clade, which was demonstrated with SSU rDNA previously (Linton et al. 2000), either groups with the five aforementioned taxa (pellicle morphology data set) or emerges as the sister to the *E. gracilis–E. stellata* clade (SSU rDNA data set) (Fig. 9). Analyses of more taxa that are morphologically similar to *L. ovata* and *P. pyrum* should shed considerable light onto the specific phylogenetic position of this group within the phototrophic euglenids.

*Evolutionary morphology of the euglenid pellicle.* Figure 10 shows pellicle character states parsimoniously mapped onto a synthetic tree. In general, there was very little homoplasy in the pellicle data set, and most nodes were supported by multiple character state changes (Figs. 6 and 10). The analyses suggest that only two character states evolved convergently:

(1) Taxa classified as either *Phacus* or *Lepocinclis* have rigid pellicles. Our analyses suggest that cell rigidity has evolved independently at least twice but probably more than three times within the phototrophic euglenids. The data support that the rigid *P. triqueter* evolved from an ancestor with a semirigid pellicle like that found in *E. tripteris*; the rigid pellicles of *P. brachykentron* and *P. oscillans* probably evolved from an ancestral pellicle similar to that found in *E. acus*. The rigid pellicles of *L. ovata* and *P. pyrum* may have evolved independently as well; how-

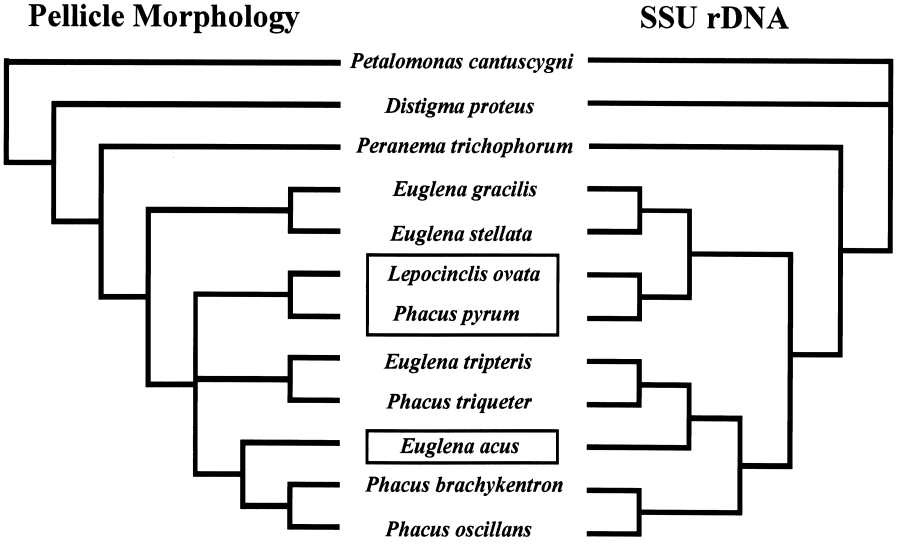


FIG. 9. Comparison of tree topologies generated from the phylogenetic analysis of morphological characters associated with the euglenid pellicle and SSU rDNA sequences. The topologies are identical except for the position of *Euglena acus* and the *Lepocinclis ovata–Phacus pyrum* clade (boxes).

ever, no extant taxon studied so far best represents the semirigid ancestral state for this lineage.

The idea of multiple independent origins of pellicle rigidity within the phototrophs makes sense from an evolutionary perspective. Euglenoid movement is quite pronounced in ancestrally colorless taxa like the phagotrophic *Peranema* and osmotrophic *Distigma*. Even though the adaptive origin of euglenoid movement remains unclear, the data clearly indicate that it occurred before the secondary origin of plastids from green algal prey (Gibbs 1978). And because plastic phagotrophs are the only euglenids that can ingest prey as large as

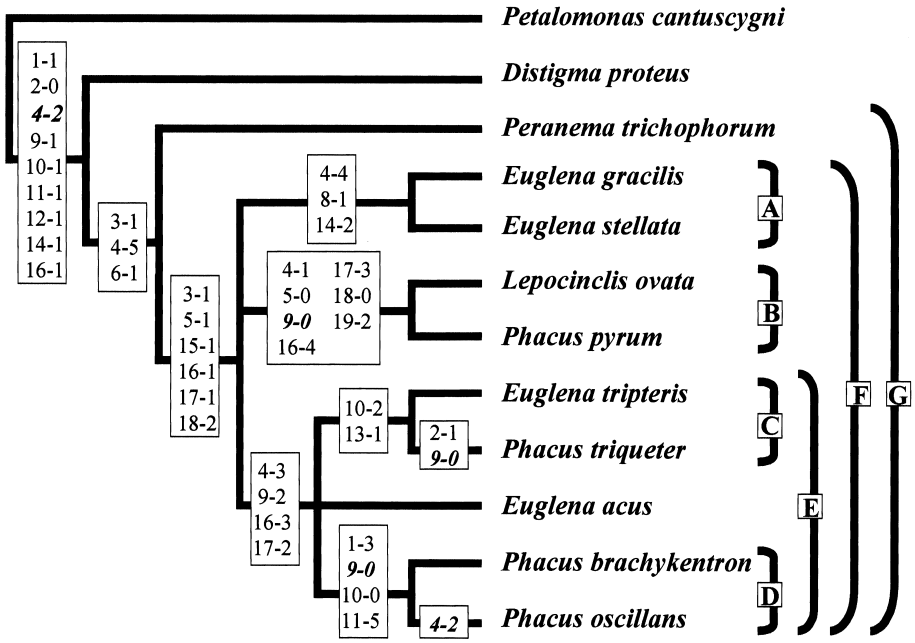


FIG. 10. Synthesis/consensus tree derived from the tree topologies shown in Figure 9. Most of the morphological character states associated with the euglenid pellicle (Table 3) have been parsimoniously mapped onto the tree. Two numbers separated by a dash represent each apomorphy; the first refers to the character and the second refers to the respective character state (Tables 3 and 4). Autapomorphies are excluded except where homoplasy has occurred (4-2 and 9-0) and where strips have become oriented clockwise (2-1). Homoplastic character states are shown in bold and italics. Seven robust clades are tagged by capital letters: (A) *Euglena*-like taxa with pellicle pores and P = 40; (B) taxa with broad strips that form doublets based on an alternation of raised and lowered articulation zones; (C) taxa with struts on the arches and a deltoid transverse cell shape; (D) rigid taxa with robust-type frames arranged longitudinally and a stubby posterior tip; (E) *Phacus*-like taxa with teethlike prearticular projections; (F) plastid-bearing taxa with a keel and strip projections; and (G) taxa with posterior strip reduction.

other eukaryotes, euglenoid movement may have been necessary for a eukaryotic plastid to have been acquired. Euglenoid movement in phototrophs, then, may be nothing more than a relict of "eukaryotrophic" ancestry. Following the origin of plastids, euglenoid movement and the associated locomotor machinery may be an unnecessary expenditure of resources, and therefore it would be evolutionarily advantageous for a phototrophic lineage to lose a plastic pellicle when possible. It appears that many separate lineages of phototrophs have done just that.

(2) Even though one state has evolved convergently (P = 18–20, the mode number of strips around the cell periphery), the value of P appears to be phylogenetically informative. For example, clade **A** is united by P = 40; clade **B** is united by P = 16; clade **E** is united by P = 32. The mode number of strips around the cell periphery of both *P. oscillans*, P = 20, and *E. acus*, P = 28, is inferred to have resulted from a permanent strip reduction event. This interpretation is supported by the range of variation of P in *E. acus*, namely 28–36, where the median is P = 32 (Table 2). Furthermore, comparative morphology suggests that a permanent strip-halving event occurred along the lineage leading to clade **B.** This interpretation is consistent with the data P = 16, $W_A$ = 0, and $W_P$ = 2, which would be the expected result after a strip-halving event from an ancestor with P = 32, $W_A$ = 1, and $W_P$ = 3 (Table 2). However, confidence in this hypothesis will remain modest until the precise position of clade **B** within the phototrophs (clade **F**) is well supported.

The most recent ancestor of taxa with strips arranged helically is inferred to have possessed a number of peripheral strips close to that found in *D. proteus*, P = 18. By inference, a permanent strip duplication event, where P jumped from about 20 to over 40, occurred in the ancestor of clade **G.** Although we parsimoniously mapped P = 50–54 at the ancestral node of clade **G**, this value may actually reflect an increase in a value of P that was ancestrally closer in value to 40; that is, this increase may have occurred independently along the lineage leading to *Peranema trichophorum.* Because P doubles just before cytokinesis, permanent strip duplication events are likely a direct consequence of an ancestral cell's failure to divide after the cytoskeletal components where already replicated. Likewise, permanent strip-halving events may be the result of an ancestral cell's failure to duplicate the pellicle strips before cytokinesis.

Clade **G** is united by the presence of strip reduction at the posterior end, which is correlated with the permanent strip duplication event described above. The pattern of strip reduction found in the taxa in clade **F** takes the form of discrete whorls; however, the taxa used in this study do not permit us to further examine the inferred polarity of all known states for $W_P$ (Leander and Farmer 2000). Nonetheless, clade **B** shares $W_P$ = 2 and clade **C** shares $W_P$ = 3. Because P = 32 and $W_P$ = 2 in *P. brachykentron*, we infer that the permanent strip reduction event in *P. oscillans*, P = 20, caused $W_P$ to decrease from two whorls to one (Fig. 5, F and G). If, as we have suggested previously, $W_P$ = 3 reduced to $W_P$ = 2 as a result of a strip-halving event in clade **B**, where P = 32 became P = 16, then ancestral whorl I must have disappeared (Table 2). Therefore, whorl I in clade B may actually be homologous to whorl II in a taxon like *E. tripteris*, which possesses the states of $W_P$ = 3 and P = 32 (Table 2).

The morphology of the euglenid posterior end varies considerably and may be, for example, rounded (e.g. *L. salina*, Conforti and Tell 1983), conical (e.g. *E. stellata*), sharp (e.g. *L. ovata*, Fig. 1), or extremely drawn out (e.g. *E. bonettoi*, Couté and Thérézien 1994). Sharp posterior ends appear to be correlated with phototrophic taxa with rigid or semirigid pellicles, whereas taxa capable of extensive euglenoid movement tend to possess posterior ends that are either rounded or more gently tapered (conical). With respect to the rigid taxa we examined, two extreme states for the morphology of the posterior end were observed, namely "sharp" and "stubby." Because the precise phylogenetic position of clade **B** is unclear, "sharp posterior end" was not mapped onto the tree (Table 3, Fig. 10). The variation in posterior tip morphology may not only be related to the degree of pellicle rigidity but a direct consequence of mechanisms associated with cytokinesis that are analogous to the phenomenon of "rotokinesis" (spinning movements of one daughter cell relative to the other facilitates separation during late cytokinesis) in dividing ciliates like *Tetrahymena* (Brown et al. 1999).

Although most taxa in this analysis possessed helically arranged strips oriented counterclockwise, *Phacus triqueter* evolved a clockwise orientation. Gojdics (1953) noted that most taxa classified as *Euglena* possess strips oriented counterclockwise, the exceptions being *E. oxyuris* Schmarda, *E. alata* Thompson, and *E. estonica* Möld. However, other euglenids have pellicle strips arranged clockwise as well, such as *E. helicoideus* Lemmer zow (Conforti and Tell 1983, 1989, B. S. Leander, personal observation). Leedale (1964) claimed that the handedness of strips even vary within taxa, with 5%–30% of the clonal *E. spirogyra* Ehrenberg cells having a clockwise orientation and the rest being counterclockwise. In contrast, we did not observe intraspecific variation for this character in any taxa. Based on these preliminary data, we suspect that the handedness of helical strips has changed multiple times during the evolution of euglenids. However, with an understanding of the way strips segregate during cytokinesis (Sommer and Blum 1965, Hofmann and Bouck 1976, Mignot et al. 1987, Bouck and Ngo 1996), it remains enigmatic how a counterclockwise orientation of pellicle strips converted to a clockwise orientation and vice versa.

The transverse shape of relaxed cells provides strong evidence for clades at different levels in the phylogeny. The data suggest that a circular transverse shape was present in the most recent common ancestor of plastic euglenids. The taxa in clade **C** possess a pronounced

deltoid shape in transverse section and the taxa in clade **D** have an ovoid shape.

Surface features of strips, aside from termination patterns, also provide important information about phylogenetic relationships. For example, the taxa in clade **A** are united by the presence of pellicle pores, and this state may mark a much larger clade, including many taxa currently classified as *Euglena*, *Colacium*, and *Trachelomonas* (Leander and Farmer 2000). The taxa in clade **C** possess struts, which are consecutive ripples in the arches that run perpendicular to the longitudinal axis of each strip. Struts have also been reported on the strips of *P. orbicularis* Hübner and *P. helicoides* Pochmann (Conforti and Tell 1989, Couté and Thérézien 1994). The struts on *E. tripteris* are present only on every alternate strip, which lends more evidence that the basic unit of the pellicle consists of strip doublets (Leander and Farmer 2001).

The substructure of strips is quite diverse among euglenids (Leander and Farmer 2001), and our analyses suggest that it is informative at many levels in the phylogenetic hierarchy (Fig. 10, Table 3). For example, euglenids with helical pellicles are also unified by the presence of an overhang, and all taxa in clade **F** possess a distinct keel between the arch and the heel. The analyses suggest that the arches became successively wider within clade **F.** The arches are roughly 2 times the width of the heels in clade **A**, the arches are over 3 times as long as the heels in clade **E**, and the arches are over 10 times the width of the heels in clade **B.** The taxa used in this analysis did not permit us to test the polarity of the states for frames; however, the frames were consistent within each of the four least inclusive clades. Clade **A** has plateau-shaped frames, clade **B** and **C** have M-shaped frames, and clade **D** and *E. acus* have robust-type frames. Because the precise phylogenetic position of *E. acus* and clade **B** remain obscure, we did not map M-shaped and robust-type frames onto the tree.

Strip doublets based on the alternation of raised and lowered articulation zones is a major apomorphy for clade **B.** This clade also possesses novel prearticular projections that were dovetailed in shape. The data suggest that threadlike prearticular projections first evolved in the ancestor of clade **F** where they subsequently became teethlike in the ancestor of clade **E.** Most taxa in clade **F** possess postarticular projections in the form of an indented plate, which is parsimoniously interpreted as being the ancestral state for the group. In this analysis, threadlike and teethlike postarticular projections are autapomorphies for *E. gracilis* and *P. brachykentron*, respectively.

*Taxonomic implications.* The taxonomic history of *Euglena*, *Phacus*, and *Lepocinclis* is fraught with indecision. For example, *P. triqueter sensu* Dujardin (1841) was once *E. triquetra sensu* Ehrenberg (1834) (Gojdics 1953). In 1883, Klebs changed *P. tripteris* to *E. tripteris*, and in Pochmann's (1942) monograph on *Phacus*, *E. tripteris* is listed as *P. tripteris.* However, more modern monographs (Gojdics 1953, Pringsheim 1956, Huber-Pestalozzi 1955) continue the name *E. tripteris.* This taxonomic indecisiveness is a natural consequence of limited morphological information and a noncladistic approach to classification. Our analyses coupled with previous phylogenetic studies of SSU rDNA (Linton et al. 1999, Linton et al. 2000, Preisfeld et al. 2000) clearly demonstrate that *Euglena*, *Phacus*, and *Lepocinclis* do not label monophyletic groups of plastid-bearing euglenids. Only after a more accurate picture of euglenid phylogeny emerges from both molecular and detailed morphological comparisons of many taxa can a classification system with predictive power be established; this classification system will most likely be founded on clades with unambiguous apomorphy-based definitions (Simpson 1997, Patterson 1999). Therefore, we attempted to demonstrate the utility of pellicle morphology in both the assessment of phylogenetic relationships and the development of clade definitions.

One consequence of this approach is that the composition of many of the currently recognized genera of phototrophic euglenids will need to be restructured or abandoned all together. It appears that *Euglena*, for instance, is complexly paraphyletic and cladistically tags a group that includes all plastid-bearing euglenids with a single emergent flagellum plus their colorless descendants (e.g. *Astasia*, *Khawkinea*, and *Cyclidiopsis*). Moreover, there are at least three robust clades that include taxa currently classified as *Phacus* and that can be clearly defined with a pellicle-based apomorphy. These are clade **B**, strip doublets based on an alternation of raised and lowered articulation zones; clade **C**, deltoid cross-sectional shape and the presence of struts; and clade **D**, longitudinal strips with a robust-type frame and a stubby posterior tip (Fig. 10). Although we refrain from doing so here, these clades will certainly warrant taxon names within a modern classification system. It is possible that the name *Phacus* can be conserved if most other *Phacus* taxa continue to group within clade **E**; however, taxa like *Phacus pyrum* may need to drop the name. It is currently unclear whether the name *Lepocinclis* will be at all meaningful within a cladistics-based taxonomic framework.

Financial support was provided by the National Science Foundation PEET (Partnerships for Enhancing Expertise in Taxonomy, grant no. DEB 4-21348). We thank C. Lewandowski for providing some of the cultures used in the study. We are grateful to E. W. Linton, P. J. P. Brown, and J. P. Shields for helpful discussions and to R. P. Witek for assistance with the collection of replicate morphological data. We also thank C. A. Leander and D. Porter for providing lab space and assistance with the generation of DNA sequences. The clarity of this manuscript was significantly enhanced by the suggestions from two anonymous reviewers.

Angeler, D. G., Müllner, A. N. & Schagerl, M. 1999. Comparative ultrastructure of the cytoskeleton and nucleus of *Distigma* (Euglenozoa). *Eur. J. Protistol.* 35:309–18.

Bouck, G. B. & Ngo, H. 1996. Cortical structure and function in euglenoids with reference to trypanosomes, ciliates, and dinoflagellates. *Int. Rev. Cytol.* 169:267–318.

Bourrelly, P & Couté, A. 1981. Ultrastructure de la cuticle de quelques eugleniens. II. *Phacus horridus* Pochmann. *Protistologica* 17:359–63.

Bricheux, G. & Brugerolle, G. 1986. The membrane cytoskeleton complex of euglenids. I. Biochemical and immunological characterization of epiplasmic proteins in *Euglena acus*. *Eur. J. Cell Biol.* 40:150–9.

Brown, J. M., Hardin, C. & Gaertig, J. 1999. Rotokinesis, a novel phenomenon of cell locomotion-assisted cytokinesis in the ciliate *Tetrahymena thermophila*. *Cell Biol. Int.* 23:841–8.

Buetow, D. E. 1968. Morphology and ultrastructure of *Euglena*. *In* Beutow, D. E. [Ed.] *The Biology of Euglena*, Vol. I. Academic Press, New York, pp. 109–84.

Bütschli, O. 1884. Protozoa. *In* Bronn's Klassen und Ordnung des Thier-Reichs 2, Abt. II Mastigophora, Leipzig, pp. 617–1097.

Calkins, G. 1933. *The Biology of the Protozoa*. Lea and Febinger, Philadelphia. 607 pp.

Cann, J. P. 1986. Ultrastructural observations of taxonomic importance on the euglenoid genera *Gyropaigne* Skuja, *Parmidium* Christen, and *Rhabdospira* Pringsheim (Euglenida: Rhabdomonadina). *Arch. Protistenkd.* 132:395–401.

Conforti, V. & Tell, G. 1983. Disposicion de las bandas y estrias de la cuticula de *Lepocinclis salina* Fritsch, (Euglenophyta) observadas en M. E. B. *Nova Hedwigia* 38:165–8.

Conforti, V. & Tell, G. 1989. Ultrastructure of the pellicle and the envelope of some euglenoid flagellates from Argentina by means of S.E.M. *Nova Hedwigia* 48:187–206.

Couté, A. & Thérézien, Y. 1994. Nouvelle contribution à l'étude des euglénophytes (Algae) de l'Amazonie bolivienne. *Nova Hedwigia* 58:245–72.

Dragos, N, Péterfi, L. S. & Popescu, C. 1997. Comparative fine structure of pellicular cytoskeleton in *Euglena* Ehrenberg. *Arch. Protistenkd.* 148:277–85.

Dubreuil, R. R. & Bouck, G. B. 1985. The membrane skeleton of a unicellular organism consists of bridged, articulating strips. *J. Cell Biol.* 101:1884–96.

Dujardin, F. 1841. *Histoire naturelle des Zoophytes Infusoires*. Roret, Paris, p. 684.

Ehrenberg, C. G. 1834. *Organization in der Richtung des kleinsten Raumes*. Phys. Abhandlung, Berlin.

Elwood, H. J., Olsen, G. J. & Sogin, M. L. 1985. The small-subunit ribosomal RNA gene sequences from hypotrichous ciliates *Oxytricha nova* and *Stylonychia pustulata*. *Mol. Biol. Evol.* 2:399–410.

Eriksson, T. 1998. AutoDecay ver. 4.0 (program distributed by the author). Bergius Foundation, Royal Swedish Academy of Sciences, Stockholm.

Farmer, M. A. 1988. *A Re-Evaluation of the Taxonomy of the Euglenophyceae Based on Ultrastructural Characteristics*. Dissertation. Rutgers, The State University of New Jersey, New Brunswick, NJ. 295 pp. Available on microfilm from University Microfilms International, Order Number 8903434.

Felsenstein, J. 1985. Confidence limits on phylogenies: an approach using the bootstrap. *Evolution* 39:783–91.

Gallo, J. M. & Shrével, J. 1982. Euglenoid movement in *Distigma proteus*. I. Cortical rotational motion. *Biol. Cell* 44:139–48.

Gibbs, S. P. 1978. The chloroplasts of *Euglena* may have evolved from symbiotic green algae. *Can. J. Bot.* 56:2883–9.

Gojdics, M. 1953. *The Genus* Euglena. The University of Wisconsin Press, Madison. 268 pp.

Hofmann, C. & Bouck, G. B. 1976. Immunological and structural evidence for patterned intussusceptive surface growth in a unicellular organism. *J. Cell Biol.* 69:693–715.

Hollande, A. 1942. Etude cytogique et biologique de quelques flagelles libres. *Arch. Zool. Exp. Gen.* 83:1–268.

Hollande, A. 1952. Classe des Eugleniens (Euglenoidina Bütschli, 1884). *Traite Zool.* 1:238–84.

Huber-Pestalozzi, G. 1955. *Das Phytoplankton des Süßwassers, Systematik und Biologie*, 4. Teil, Euglenophyceen. E. Schweizerbart'sche Verlagsbuchhandlung, Unveränderter Nachdruck, pp. 601–1135.

Kirk, J. T. O. & Juniper, B. E. 1964. The fine structure of the pellicle of *Euglena gracilis*. *J. R. Micro. Soc.* 82:205–10.

Klebs, G. 1883. Ueber die Organization einiger Flagellatengruppen und ihre Beziehungen zu Algen und Infusorien. *Unter. Botan. Inst. Tübingen* 1:233–362.

Leander, B. S. & Farmer, M. A. 2000. Comparative morphology of the euglenid pellicle. I. Patterns of strips and pores. *J. Eukaryot. Microbiol.* 47:469–79.

Leander, B. S. & Farmer, M. A. 2001. Comparative morphology of the euglenid pellicle. II. Diversity of strip substructure. *J. Eukaryot. Microbiol.* 48(2):204–19.

Leedale, G. F. 1964. Pellicle structure in *Euglena*. *Br. Phycol. Bull.* 2:291–306.

Leedale, G. F. 1967. *Euglenoid Flagellates*. Prentice Hall, Englewood Cliffs, NJ. 242 pp.

Leedale, G.F. 1978. Phylogenetic criteria in euglenoid flagellates. *Biosystems* 10:183–7.

Leedale, G. F. 1985. Order 3. Euglenida. *In* Lee, J. J., Hutner, S. H. & Bovee, E. C. [Eds.] *The Illustrated Guide to the Protozoa*. Society of Protozoologists, Kansas, pp. 41–54.

Leedale, G. F. & Hibberd, D. J. 1974. Observations on the cytology and fine structure of the euglenoid genera *Menoidium* Perty and *Rhabdomonas* Fresenius. *Arch. Protistenkd.* 116:319–45.

Lefort-Tran, M., Bre, M. H., Ranck, J. L. & Pouphile, M. 1980. *Euglena* plasma membrane during normal and vitamin $B_{12}$ starvation growth. *J. Cell Sci.* 41:245–61.

Lemmermann, E. 1913. "Eugleninae" in Die Süsswasserflora Deutschlands, sterreichs, und der Schweiz. *Jena* 2:115–74.

Linton, E. W., Hittner, D., Lewandowski, C., Auld, T. & Triemer, R. E. 1999. A molecular study of euglenoid phylogeny using small subunit rDNA. *J. Eukaryot. Microbiol.* 46:217–23.

Linton, E. W., Nudelman, A., Conforti, V. & Triemer, R. E. 2000. A molecular analysis of the genus *Euglena* (Euglenophyta) using SSU rDNA. *J. Phycol.* 36:740–6.

Mignot, J. P. 1965. Ultrastructure des eugléniens. I. Étude de la cuticle chez différentes espéces. *Protistologica* 1:5–15.

Mignot, J. P., Brugerolle, G. & Bricheux, G. 1987. Intercalary strip development and dividing cell morphogenesis in the euglenid *Cyclidiopsis acus*. *Protoplasma* 139:51–65.

Montegut-Felkner, A. E. & Triemer, R. E. 1997. Phylogenetic relationships of selected euglenoid genera based on morphological and molecular data. *J. Phycol.* 33:512–9.

Patterson, D. 1999. The diversity of eukaryotes. *Am. Nat.* 154:96–124.

Perty, M. 1849. Über Verticale verbreitung mikroskopischer Lebensformen. *Mitt. Naturforsch. Gesellsh. Bern* 146–149:17–45.

Pochmann, A. 1942. Synopsis der Gattung *Phacus*. *Arch. Protistenkd.* 95:81–252.

Preisfeld, A., Berger, S., Busse, I., Liller, S. & Ruppel, H.G. 2000. Phylogenetic analysis of various euglenoid taxa (Euglenozoa) based on 18S rDNA sequence data. *J. Phycol.* 36:220–6.

Pringsheim, E. G. 1956. Contributions toward a monograph of the genus *Euglena*. *Nova Acta Leopoldina* 18:1–168.

Rambaut, A. 1996. Sequence Alignment Editor ver. 1.0 alpha 1 (program available from: http://evolve.zoo.ox.ac.uk/Se-Al/Se-Al.html). University of Oxford, Oxford.

Schwelitz, F. D., Evans, W. R., Mollenhaur, H. H. & Dilley, R. A. 1970. The fine structure of the pellicle of *Euglena gracilis* as revealed by freeze-etching. *Protoplasma* 69:341–9.

Senn, C. 1900. Euglenineae. *Die Nat. Pflanzen*. 1:173–85.

Simpson, A. G. B. 1997. The identity and composition of the Euglenozoa. *Arch. Protistenkd.* 148:318–28.

Sommer, J. R. & Blum, J. J. 1965. Cell division in *Astasia longa*. *Exp. Cell Res.* 39:504–27.

Starr, R. C. & Zeikus, J. A. 1993. UTEX—The Culture Collection of Algae at the University of Texas at Austin, 1993 List of Cultures. *J. Phycol.* 29:1–106.

Suzaki, T. & Williamson, R. E. 1985. Euglenoid movement in *Euglena fusca*: evidence for sliding between pellicular strips. *Protoplasma* 124:137–46.

Swofford, D. L. 1999. PAUP*: Phylogenetic analysis using parsimony (and other methods), version 4.0. Sinauer Associates, Sunderland, MA.

Tell, G. & Conforti, V. 1986. Euglenophyta pigmentadas de la Argentina. *Bibl. Phycol.*, Berlin, Stuttgart, 301 pp.

Thompson, J. D., Gibson,T. J., Plewniak, F., Jeanmougin, F. & Higgins, D. G. 1997. The ClustalX windows interface: flexible strategies for multiple sequence alignment aided by quality analysis tools. *Nucleic Acids Res.* 24:4876–82.

Triemer, R. E. & Farmer, M. A. 1991. The ultrastructural organization of the heterotrophic euglenids and its evolutionary implications. *In* Patterson, D. J. & Larsen, J. [Eds.] *The Biology of Free-living Heterotrophic Flagellates*. Clarendon Press, Oxford, pp.185–204.

Van de Peer, Y., Robbrecht, E., de Hoog, S., Caers, A. De Rijk, P. & De Wachter, R. 1999. Database on the structure of small subunit ribosomal RNA. *Nucleic Acids Res.* 27:179–83.

Zakrys, B. & Walne, P. L. 1994. Floristic, taxonomic and phytogeographic studies of green Euglenophyta from the Southeastern United States, with emphasis on new and rare species. *Algol. Stud.* 72:71–114.

Zolan, M. E. & Pukkila, P. J. 1986. Inheritance of DNA methylation in *Coprinus cinereus*. *Mol. Cell. Biol.* 6:195–200.